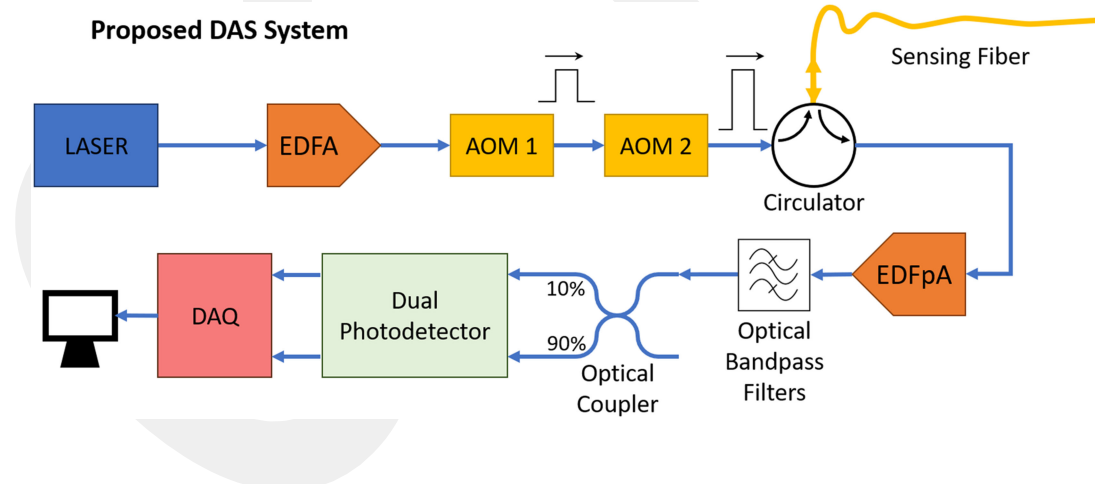


# A Direct Detection Fiber Optic Distributed Acoustic Sensor With a Mean SNR of 7.3 dB at 102.7 km

Volume 11, Number 6, December 2019

Faruk Uyar  
Talha Onat  
Canberk Unal  
Tolga Kartaloglu  
Ekmel Ozbay, *Senior Member, IEEE*  
Ibrahim Ozdur, *Member, IEEE*



DOI: 10.1109/JPHOT.2019.2948211

# A Direct Detection Fiber Optic Distributed Acoustic Sensor With a Mean SNR of 7.3 dB at 102.7 km

Faruk Uyar<sup>1</sup>,<sup>1</sup> Talha Onat,<sup>1</sup> Canberk Unal,<sup>1</sup> Tolga Kartaloglu,<sup>1</sup>  
Ekmel Ozbay<sup>1,2,3</sup>,<sup>1,2,3</sup> Senior Member, IEEE,  
and Ibrahim Ozdur,<sup>4</sup> Member, IEEE

<sup>1</sup>Nanotechnology Research Center, Bilkent University, Ankara 06800, Turkey

<sup>2</sup>Department of Electrical and Electronics Engineering, Bilkent University, Ankara 06800, Turkey

<sup>3</sup>Department of Physics, Bilkent University, Ankara 06800, Turkey

<sup>4</sup>Department of Electrical and Electronics Engineering, Abdullah Gul University, Kayseri 38080, Turkey

DOI:10.1109/JPHOT.2019.2948211

This work is licensed under a Creative Commons Attribution 4.0 License. For more information, see <https://creativecommons.org/licenses/by/4.0/>

Manuscript received August 26, 2019; revised October 10, 2019; accepted October 15, 2019. Date of publication October 18, 2019; date of current version November 13, 2019. This work was partially supported by The Scientific and Technological Research Council of Turkey (TUBITAK) under Grant 3190696 and ASELSAN A.Ş. Corresponding author: Faruk Uyar (e-mail: faruk.uyar@bilkent.edu.tr).

**Abstract:** In this work, we present the experimental results of a direct detection  $\varphi$ -OTDR based distributed acoustic sensor system. The system uses two cascaded acousto-optic modulators in order to generate optical pulses with very high extinction ratio and dual photodetector scheme for high dynamic range. The proposed schemes are investigated in detail and their performance enhancement is experimentally verified. Four piezoelectric based fiber stretchers are placed on a  $\sim 104$  km single-mode test fiber at the distances of 1 km, 10 km, 87 km and 102.7 km and used for perturbation tests. The stretchers generated vibration signals which are analyzed to quantify the system performance. The signal-to-noise ratio (SNR) of vibration signals at the monitored distances is measured over the 12-hour recorded data within 34-second time windows considering the multi-point random interference of scattered light and fading phenomena. Using the 12-hour data, SNR histograms at four different locations are generated and mean SNR values are obtained. The signals received from 102.7 km has a maximum SNR of 24.7 dB and a mean SNR of 7.3 dB with a spatial resolution of 15 m. To the best of our knowledge, this is the highest-range reported direct detection  $\varphi$ -OTDR based distributed acoustic sensor system.

**Index Terms:** Optical sensors, Rayleigh scattering, phase sensitive optical time domain reflectometry, fiber optic systems.

## 1. Introduction

The security of long-distance structures such as pipelines and borders is a challenging problem and requires expensive solutions. In the last few decades, phase sensitive optical time domain reflectometry ( $\varphi$ -OTDR) technology based distributed acoustic sensing (DAS) systems has been drawing more and more attention as a cost-effective solution to the problem [1], [2].  $\varphi$ -OTDR systems are originally developed from OTDR systems where the Rayleigh backscattered signal intensity from a fiber optic cable only depends on the distance [3]. However, with the use of highly coherent light sources, the backscattered coherent light within the optical pulse interferes and results in an intensity

profile related to the phase difference of the interfering light signals. The main difference between the OTDR and  $\varphi$ -OTDR sensors is the linewidth (or coherence length) of the light source. In  $\varphi$ -OTDR systems the intensity profile difference at any location gives information about the relative phase difference within the optical pulse which mainly results from external acoustic signals.

There are different optical interrogation approaches that offer different system performances. One approach uses direct detection  $\varphi$ -OTDR system and reaches to 50 km range [4]. Another approach uses counter pumping fiber distributed Brillouin amplification and can detect vibration signals over a 124 km fiber optic cable [5]. Another technique again uses counter pumping optical amplification (Raman Amplification) and has a range of 131 km [6]. Both of these methods use counter pumping to get effective optical amplification at the end of the sensing fiber. However, it is not always practical to reach to the other end of the fiber and install a second optical component.

The  $\varphi$ -OTDR systems can be divided into two sub categories depending on the detection scheme, namely coherent detection [7] and direct detection [8]. Here, we focus on direct detection technique due to the simpler design and lower cost. In this work, we propose a direct detection  $\varphi$ -OTDR system and present experimental results. In the proposed scheme, dual acousto-optic modulators (AOM) are used in order to minimize the coherent noise [9] generated by the leaked continuous light wave from the modulators which makes it challenging to realize long-distance event detection along the sensing fiber. The use of dual AOMs increases the extinction ratio (ER) of the generated optical pulses to higher than 100 dB which is essential for the long-distance measurement of the  $\varphi$ -OTDR system [10], [11]. With this level of extinction, the optical noise level caused by the optical fluctuations becomes lower than the other noise sources (amplified spontaneous emission and thermal noise). Another challenge for ultra-long-range direct detection systems is the necessity of very high dynamic range. We propose to use a dual photo detection receiver architecture to solve this issue. In our approach, the return signal from the fiber optic sensor cable is split into two using an optical coupler with 10/90 coupling ratio. The system uses the fiber branch with higher optical power (90%) for analyzing the far away channels and uses the other fiber branch (10%) for close-in channels. With this method we eliminated the signal saturation and blurring of close-in channels.

To verify the performance enhancement of the proposed schemes, we collected datasets from the constructed  $\sim 104$  km-length test fiber. Specifically located fiber stretchers (PZT) along the test fiber were run to generate disturbances. We analyzed the frequency response of the collected data and calculated signal-to-noise ratio (SNR) of the vibration signal at the signal frequency. Measuring the SNR of a  $\varphi$ -OTDR system is not straightforward due to the signal fading and time varying response of the system hence we measured the mean SNR as described in [12] and [13]. Our results show that the proposed system has a mean SNR of 7.3 dB at 102.7 km.

## 2. Experimental Set-up

The experimental set-up of the direct detection  $\varphi$ -OTDR system is shown in Fig. 1. An ultra-narrow linewidth (100 Hz) laser operating at 1550.12 nm is used as the light source. The laser output is amplified via a booster erbium doped fiber amplifier (EDFA), with maximum output power of 1 W, and then modulated using dual AOMs, which have low insertion loss around 1.8 dB, resulting in a frequency shift of 220 MHz with respect to the input light. The AOMs generate interrogation pulses at  $\sim 1$  kHz repetition rate and 150 ns width. The optical pulse width is measured using an oscilloscope after the dual AOMs to be certain of 150 ns width without pulse clipping or distortion. The generated pulses are launched into the test fiber via an optical circulator. The Rayleigh backscattered optical signal from the fiber is directed to the detection scheme where it is amplified by a 40 dB gain erbium doped fiber pre-amplifier (EDFpA), which has a noise figure of as low as 4.0 dB. It, then, passes through a number of optical band pass filters, the narrowest of which is around 2 GHz, in order to minimize the amplified spontaneous emission in order to minimize the amplified spontaneous emission (ASE) noise of the EDFpA. The filtered optical signal is then split into two using a 10/90 optical coupler. The 10% and 90% branches of the coupler are used for monitoring the close-in and far away distances, respectively. The divided backscattered power is received by two separate photodetector (PD) units comprising low leakage InGaAs photodiodes with 0.08 nA dark current

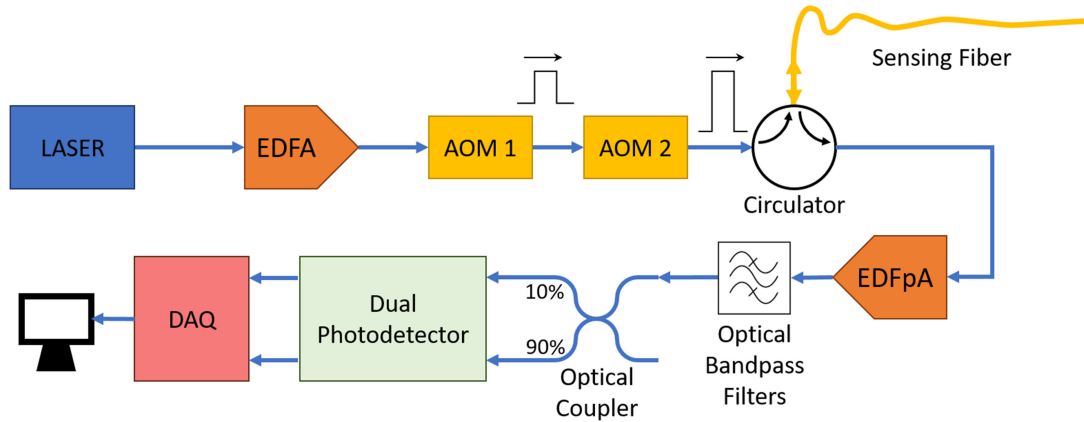


Fig. 1. Diagram of the experimental set up.

and highly-linear low-noise transimpedance amplifiers (TIA). The output electrical signals from the PD's are acquired and digitized by a data acquisition card (DAQ). Finally, the raw data is transmitted to a PC for further process.

The addition of cascaded dual AOM and dual PD techniques (details are given in the following sections) is the key design feature to achieve  $>100$  km range vibration detection. Moreover, ultra-narrow optical bandpass filters used after EDFpA for suppression of the ASE noise and also ultra-high sensitivity linear-gain TIA units after PD's considerably contribute to SNR and range improvement.

### 2.1 Dual AOM Technique and Investigation

The coherent noise, resulting from the finite extinction ratio (also known as pulse on/off ratio) of the optical pulses, is one of the most important factors that limits the SNR performance and sensing range in a  $\varphi$ -OTDR based DAS system [10]. Commercial AOMs employed in the experimental configuration have extinction ratio (ER) values around 50 to 65 dB. Therefore, even when AOM is turned off, a certain amount of continuous wave (CW) light leaks into the fiber. The leaked CW component gets backscattered from the fiber and causes a background noise level. It also experiences multi-point random coherent interference in the fiber, resulting in trace fluctuations in the signal, which can be referred to as intra-band noise [11] and can be expressed as;

$$P_{\text{int}}(z) = 2\sqrt{P_p \alpha_R \frac{cT_P}{2n} e^{-2\alpha z} \frac{P_{CW} \alpha_R (1 - e^{-2\alpha L})}{\alpha}} \quad (1)$$

where  $P_p$  and  $P_{CW}$  are the pulse peak power and CW leakage power of incident light, respectively.  $\alpha_R$  is the Rayleigh backscattering coefficient,  $c$  is the speed of light in the vacuum,  $T_P$  is the pulse duration,  $L$  is the length of the sensing fiber,  $n$  and  $\alpha$  are the refractive index and attenuation coefficient of the fiber.  $z$ , here, denotes the position along the fiber and it implies that the ratio of the noise caused by the leaked CW light to the signal itself gets larger in the far away distances, which yields lower SNR.

Formula (1) indicates that the coherent noise problem becomes more critical for far distances since the backscattered CW component accumulates over the fiber length. The longer fiber leads to higher intra-band noise level that blurs the backscattering traces. Thus, the coherent noise becomes the major limiting factor for long range measurements. In order to increase the ER and minimize the coherent noise [9], dual AOM architecture is used. For this purpose, two cascaded AOMs were synchronized and an appropriate delay is inserted between the control pulses considering the optical delay between the AOMs as shown in Fig. 2. With this technique, 150 ns optical pulses with ER of  $>110$  dB is obtained.

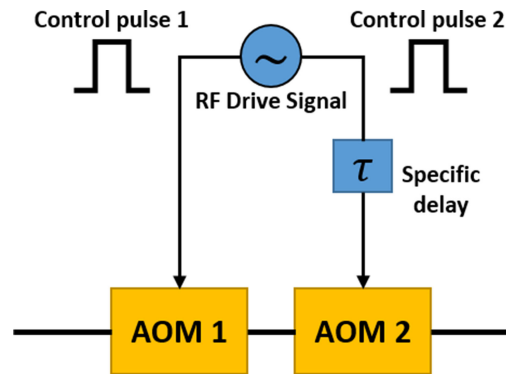


Fig. 2. An illustration of dual AOM structure.

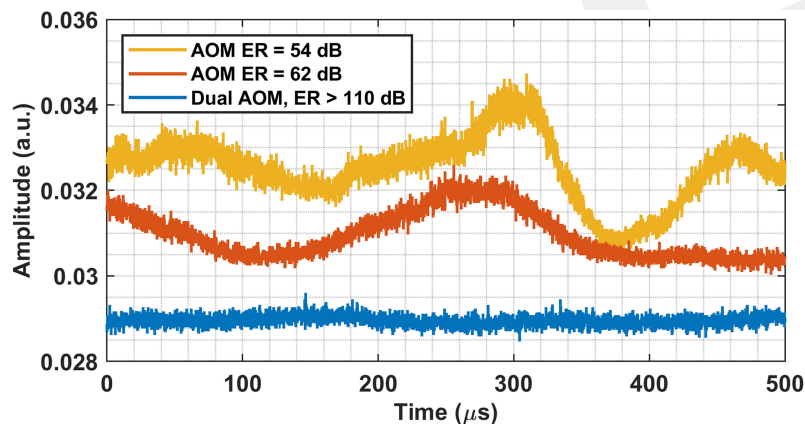


Fig. 3. Time domain data for three cases of AOM ER.

We investigated the effect of AOM ER in the  $\varphi$ -OTDR system by observing the Rayleigh backscattering light of the leaked signal for three different cases: using single AOMs with 54 dB ER, 62 dB ER, and using two cascaded AOMs with > 110 dB ER. In the setup, the leaked signal was sent to a 50 km fiber optic cable, placed into an acoustically isolated box without a fiber stretcher. To better distinguish the fluctuations, interrogation pulses were turned off and only the background optical signal, which was caused by the leaked signal, was observed. Fig. 3 shows the return signal behavior in time domain for three different cases. It can be seen that lower ER leads to more fluctuation in the traces. The intra-band noise level induced by the CW leakage goes down as the ER increases and disappears in the case of dual cascaded AOMs.

## 2.2 Dual PD Technique and Investigation

Since the received light from the far distances is very weak in  $\varphi$ -OTDR systems, the pump current of the EDFPA has to be maximized to obtain enough signal power. On the other hand, with high EDFPA gain the light received from close-in distances would be amplified too much that the photoreceiver saturation may occur in those regions. This saturation effect may blind the close-in channels in the trace and reduce the visibility in the  $\varphi$ -OTDR interference pattern, making it difficult to detect and measure dynamic events. To overcome this problem, the light power is divided by a 10/90 coupler after the OBPFs and given to two separate PD's that are connected to two arms of the coupler, respectively. 90% of the light is used for monitoring the far distances, and 10% of the light is used for monitoring the close-in distances. The traces obtained from two PD's are split at the location where the saturation of the 90% branch ends and then the first segment of the first PD trace and the

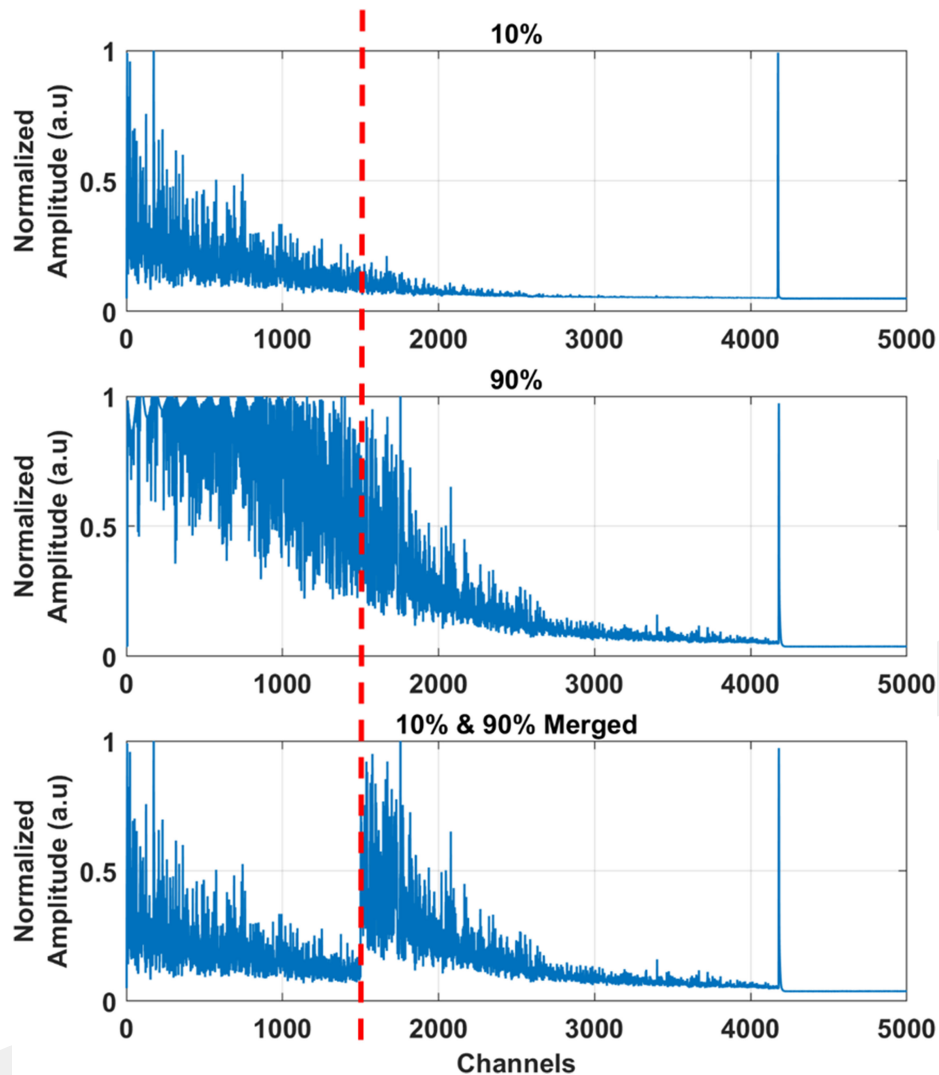


Fig. 4. Dual PD raw data signal form.

second segment of the second PD trace are concatenated into a single trace as shown in Fig. 4. This figure shows the Rayleigh backscattering traces for 10% and 90% of the reflected power which are obtained from a  $\sim 41$  km test fiber for demonstration purposes. The observed saturation at the 90% branch of the photoreceiver occurs in the electronic domain in which the TIA circuitry limits the output voltage level to ensure the full-range operation as well as damage protection.

### 3. Experimental Results With $\sim 104$ km Test Fiber

The performance tests of the direct detection  $\varphi$ -OTDR system, shown in Fig. 1, were performed using  $\sim 104$  km test fiber with four piezo based fiber stretchers. The details of the test fiber and perturbation tests are given in the following sections.

#### 3.1 Test Fiber and Parameter Determination

For the perturbation tests a  $\sim 104$  km test fiber with PZT's were used. PZT's are fiber wound piezoelectric elements for inducing external vibration events that contain  $\sim 12$  m of fiber which were

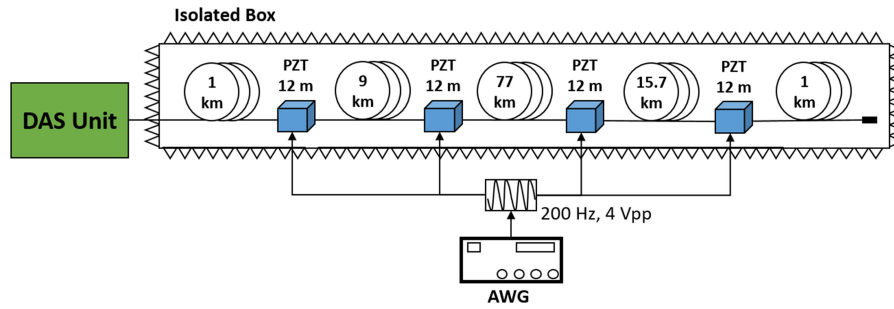


Fig. 5. 103.4 km length test fiber.

TABLE 1  
Test Parameters

Interrogation period ( $T_P$ )	Repetition rate ( $f_r$ )	Pulse duration ( $\Delta T$ )	Spatial resolution	Pulse peak power
1040 $\mu$ s	962 Hz	150 ns	15 m	200 mW

subjected to dynamic vibration events. The test fiber, shown in Fig. 5, was 103.4 km long single-mode fiber (SMF-28). Four PZT's were placed at the positions of 1 km, 10 km, 87 km and 102.7 km as the vibration sources. Their positions were specifically chosen in this manner so that the close-in and far channels could be monitored at the same time provided by the dual PD scheme. The fiber coils were placed in an acoustically isolated box in the laboratory. The PZT's were driven using an arbitrary waveform generator (AWG) located outside the box.

Parameters of the system were determined by the length of the fiber and the desired optical resolution. Interrogation period, and thereby repetition rate, is limited by the length of the test fiber and must be greater or equal to the optical pulse round-trip time, i.e.,  $T_p \geq \tau$ . It yields,

$$T_p \geq \frac{2Ln}{c} \cong 1034 \mu\text{s} \rightarrow T_p = 1040 \mu\text{s} \Rightarrow f_r = \frac{1}{T_p} \cong 962 \text{ Hz}$$

where  $L$  is the length of test fiber,  $n$  is the refractive index of SMF-28,  $c$  is the speed of light inside vacuum and  $f_r$  is the repetition rate of the pulses.

Also, the desired resolution,  $\Delta z$ , is 15 m. The corresponding pulse duration,  $\Delta T$ , is calculated as

$$\Delta T = \frac{2n\Delta z}{c} \cong 150 \text{ ns}$$

With regard to the power of the probe pulses launched into the fiber, it should be increased to obtain larger amount of back-reflected signal, therefore higher SNR. The primary limiting factor, however, is the non-linear effects such as self-phase modulation (SPM), four-wave mixing (FWM), modulation instability (MI) and so on for the increased pulse peak power. The influences of these effects on the performance of the  $\varphi$ -OTDR are studied in detail in reference [14]. The peak power of the probe pulses is optimized to  $\sim 200$  mW in order not to degrade performance due to non-linear effects.

The complete list of parameters is given in Table 1.

### 3.2 Perturbation Tests and Results

After the test parameters were determined, a sinusoidal signal at 200 Hz and 4 Vpp was applied to all of four PZT's simultaneously. For this test, the slow-time axis interference signals at PZT locations were reconstructed by extracting the corresponding data points from the fast-time axis traces [15].

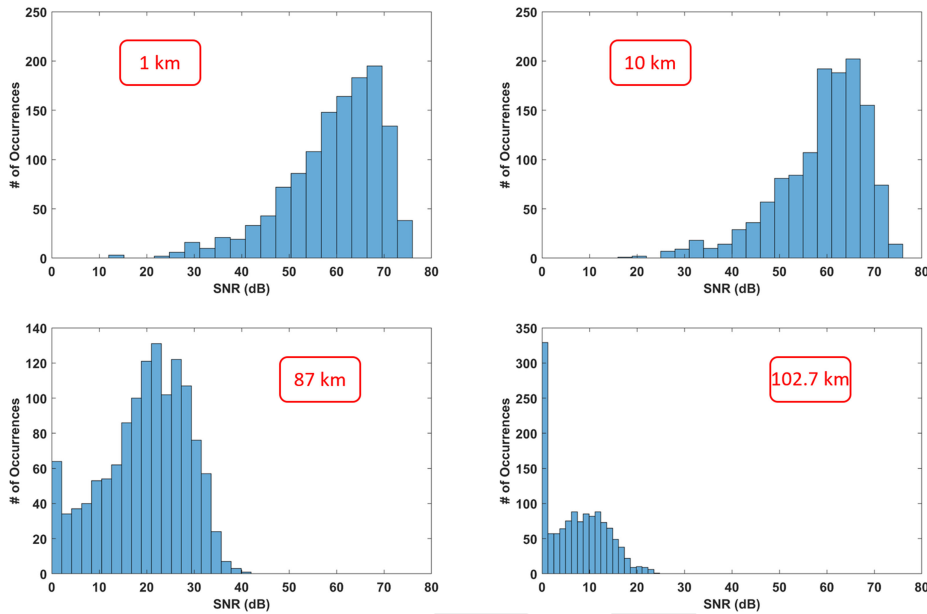


Fig. 6. SNR Histograms at the distances of 1 km, 10 km, 87 km and 102.7 km.

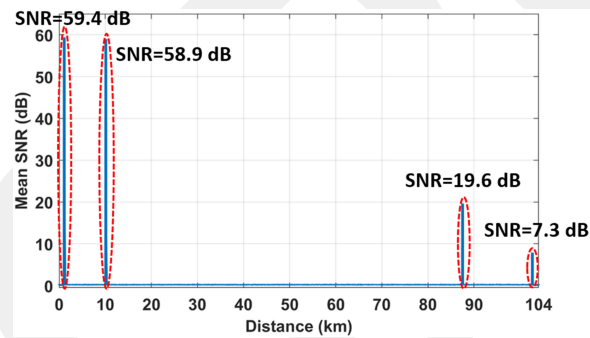


Fig. 7. Mean SNR versus distance along the test fiber.

To characterize the performance of the system at the monitored distances, we calculated the SNR of the vibration signal as the magnitude ratio of the 200 Hz peak to the background noise level,  $SNR = 10 \log(P_{signal}/P_{noise})$ , with  $2^{15}$  FFT points. Considering the random nature of multi-point coherent interference of the scattered light in fiber and fading phenomena, we collected a 40 million-sample long set of data, corresponding to  $\sim 12$ -hour record time. We measured the SNR values over  $2^{15}$ -length frames, which correspond to  $\sim 34$ -second time windows, resulting in 1281-element SNR arrays for each PZT position. We then used the arrays to generate SNR histograms at the monitored distances, as shown in Fig. 6, to quantify the performance of the system in a statistical manner, which is discussed in detail in our previous work [12].

The histograms show that the SNR does not take a single value for the applied perturbation signal, but instead it varies around a mean value, due to the fading effects and time varying response of the system. It can be seen that as the distance gets smaller, i.e., towards the launching-end of the fiber, the peak amplitudes of the fundamental frequency become stronger and yield to higher SNR. However, SNR does not keep increasing beyond a physically limited value, resulting in similar SNR histograms for both the distances of 1 km and 10 km. Also, it can be observed that weakening Rayleigh signal and increasing background noise towards the far-end of the fiber shift the histograms to lower values. Increasing number of occurrences of SNR around 0 dB in the 87 km and 102.7 km histograms demonstrates the existence of complete fading in far distances.

We calculated the mean SNR values at different PZT locations using the histograms. The calculated mean SNR values obtained from the direct measurement are plotted as a function of distance along the entire fiber of 104 km as shown in Fig. 7. According to the results, the system is verified to be capable of sensing the vibration events at the distance of 102.7 km and providing a mean SNR of 7.3 dB and maximum SNR of 24.7 dB.

#### 4. Conclusion

In this paper, we have proposed an ultra-long-distance fiber optic distributed acoustic sensing system which uses dual acousto-optic modulator and dual photodetector techniques. The dual acousto-optic modulator scheme has allowed us to minimize the coherent noise by the generation of optical pulses with  $>110$  dB extinction ratio and the dual photodetector scheme has helped us to observe the close-in and far away channels without any saturation. We have measured the SNR distributions at the distances of 1 km, 10 km, 87 km and 102.7 km; the mean SNR values are 59.4 dB, 58.9 dB, 19.6 dB and 7.3 dB, respectively. The system can have a maximum SNR of 24.7 dB and a mean SNR of 7.3 dB at 102.7 km with a spatial resolution of 15 m. These results reveal the longest direct detection DAS system reported up to date to the best of our knowledge, without using Raman pumping or hybrid amplification approaches.

The system shows its potentiality to be effectively utilized for long assets monitoring and intrusion detection in a wide range of applications such as long-distance pipeline monitoring, submarine fiber optic cable security, borderline security and so on.

---

#### References

- [1] H. F. Taylor and C. E. Lee, "Apparatus and method for fiber optic intrusion sensing," US Patent 5 194 847, Mar. 16, 1993.
- [2] J. Park, W. Lee, and H. F. Taylor, "Fiber optic intrusion sensor with the configuration of an optical time-domain reflectometer using coherent interference of Rayleigh backscattering," in *Optical and Fiber Optic Sensor Systems*, vol. 3555. Bellingham, WA, USA: Int. Soc. Opt. Eng., 1998, pp. 49–56.
- [3] A. Hartog and M. Gold, "On the theory of backscattering in single-mode optical fibers," *J. Lightw. Technol.*, vol. 2, no. 2, pp. 76–82, Apr. 1984.
- [4] G. L. Duckworth and E. M. Ku, "Optasense distributed acoustic and seismic sensing using cots fiber optic cables for infrastructure protection and counter terrorism," *Proc. SPIE*, vol. 8711, 2013, Art. no. 87110G.
- [5] J. Li *et al.*, "124 km phase-sensitive OTDR with Brillouin amplification," *Proc. SPIE*, vol. 9157, 2014, Art. no. 91575Z.
- [6] F. F. Peng, H. Wu, X.-H. Jia, Y.-J. Rao, Z.-N. Wang, and Z.-P. Peng, "Ultra-long high-sensitivity  $\varphi$ -otdr for high spatial resolution intrusion detection of pipelines," *Opt. Exp.*, vol. 22, no. 11, pp. 13804–13810, 2014.
- [7] Y. Lu, T. Zhu, L. Chen, and X. Bao, "Distributed vibration sensor based on coherent detection of phase-OTDR," *J. Lightw. Technol.*, vol. 28, no. 22, pp. 3243–3249, Nov. 2010.
- [8] J. C. Juarez, E. W. Maier, K. N. Choi, and H. F. Taylor, "Distributed fiber-optic intrusion sensor system," *J. Lightw. Technol.*, vol. 23, no. 6, pp. 2081–2087, Jun. 2005.
- [9] H. F. Martins, S. Martin-Lopez, P. Corredera, M. L. Filograno, O. Frazão, and M. González-Herráez, "Coherent noise reduction in high visibility phase-sensitive optical time domain reflectometer for distributed sensing of ultrasonic waves," *J. Lightw. Technol.*, vol. 31, no. 23, pp. 3631–3637, Dec. 2013.
- [10] C. Baker, B. Vanus, M. Wuilpart, L. Chen, and X. Bao, "Enhancement of optical pulse extinction-ratio using the nonlinear Kerr effect for phase-OTDR," *Opt. Exp.*, vol. 24, no. 17, pp. 19424–19434, 2016.
- [11] M. Ren, D.-P. Zhou, L. Chen, and X. Bao, "Influence of finite extinction ratio on performance of phase-sensitive optical time-domain reflectometry," *Opt. Exp.*, vol. 24, no. 12, pp. 13 325–13 333, 2016.
- [12] F. Uyar, T. Kartaloglu, I. Ozdur, and E. Ozbay, "Field test and fading measurement of a distributed acoustic sensor system over a 50 km-long fiber," *Proc. SPIE*, vol. 10654, 2018, Art. no. 106540D.
- [13] H. Gabai and A. Eyal, "On the sensitivity of distributed acoustic sensing," *Opt. Lett.*, vol. 41, no. 24, pp. 5648–5651, 2016.
- [14] E. T. Nesterov *et al.*, "Experimental study of influence of nonlinear effects on phase-sensitive optical time-domain reflectometer operating range," *J. Phys.: Conf. Ser.*, vol. 584, 2015, Art. no. 012028.
- [15] L. B. Liokumovich, N. A. Ushakov, O. I. Kotov, M. A. Bisyarin, and A. H. Hartog, "Fundamentals of optical fiber sensing schemes based on coherent optical time domain reflectometry: Signal model under static fiber conditions," *J. Lightw. Technol.*, vol. 33, no. 17, pp. 3660–3671, Sep. 2015.